Observed changes in stratospheric circulation: Decreasing lifetime of N_2O, 2005-2021

Michael J. Prather[1], Lucien Froidevaux[2], Nathaniel J. Livesey[2]

[1]Earth System Science Department, University of California Irvine; Irvine, CA 92697-3100, USA
5   [2]Jet Propulsion Laboratory, California Institute of Technology; Pasadena, CA 91011, USA

Correspondence to: Michael Prather (mprather@uci.edu)

Abstract. Using Aura Microwave Limb Sounder satellite observations of stratospheric nitrous oxide (N_2O), ozone, and temperature from 2005 through 2021, we calculate the atmospheric lifetime of N_2O to be decreasing~~. Because~~ at a rate of -2.1±1.2 %/decade. This
10   decrease is occurring because the N_2O abundances in the middle tropical stratosphere, where ~~it~~N_2O is photochemically destroyed, ~~increased~~are increasing at a faster rate than the bulk ~~N_2O~~N_2O in the lower atmosphere~~, the lifetime is becoming shorter.~~. The cause appears to be a more vigorous stratospheric circulation, which models predict ~~to~~as a result ~~from~~of climate change. If this climate-driven circulation trend continues to 2100, then anthropogenic N_2O
15   emissions will be removed 20% faster than current projections, and their impact on global warming and ozone depletion will be proportionately lessened. ~~This~~Because global warming is caused in part by N_2O, this finding is an example of a ~~distinct~~ negative~~, but relatively minor,~~ climate-chemistry feedback.

20   ## 1 Introduction

Projections of climate change include the acceleration of the stratospheric overturning circulation over the 21st century (Abalos et al., 2021). This three-dimensional circulation, condensed into a two-dimensional framework called the Brewer-Dobson Circulation (BDC),
25   brings tropospheric air into the tropical stratosphere where it ascends, being photochemically processed with ultraviolet radiation that increases with altitude, mixes across latitudes, and then descends at mid- to high-latitudes, re-entering the troposphere around mid-latitudes (Plumb and Mahlman, 1987; Neu and Plumb, 1999; Butchart, 2014). Observational metrics for an enhanced BDC are based on trends in the Age-of-Air (AoA) using surrogate gases
30   such as SF_6~~, but these~~. While models predict an enhanced BDC, the SF_6 observations ~~run counter to the climate model projections~~indicate an unchanged or decreasing BDC, but with large uncertainty (Karpechko et al., 2018; Abalos et al., 2021; Garney et al., 2022~~), in part because the~~). The comparison of models and measurements of AoA has proven difficult

(Fritsch et al., 2020). The search for BDC change with AoA has missed a more obvious and compelling case based on the important greenhouse gas nitrous oxide (N_2O), where recent work has shown agreement in upper stratospheric trends across satellite instruments and a model (Froidevaux et al., 2022). Here we take the Aura MLS observations of N_2O, ozone (O_3), and temperature (T) from 2005 through 2021 and show that N_2O increases through the middle tropical stratosphere, relatively greater than the rate of tropospheric increases, lead to a shorter atmospheric lifetime, an important consequence of a more vigorous BDC.

Consequences of an enhanced BDC often focushave recently focussed on the increased flux of stratospheric ozone (O_3) into the troposphere with subsequent increase in tropospheric O_3, see discussion in (Karpechko et al., 2018; Garney et al., 2022). Enhanced BDC also leads to shorter lifetimes for gases like nitrous oxide (N_2O) and chlorofluorocarbons (CFCs) as greater abundances are pushed higher in the tropical stratosphere where they experience greater photolytic destruction. Two decades ago this mechanism was proposed by Butchart and Scaife (2000) for the CFCs based on dynamical diagnostics of the BDC from a climate model. Now we have observed and quantified this effect for a major greenhouse gas. Using the simultaneous MLS vertical profiles of N_2O, O_3, and temperature, we calculate the total loss of N_2O in the column, needing only the solar spectrum and absorption cross sections, as in Prather et al. (2015, hence P2015). We find that the stratospheric N_2O loss rate is increasing faster than the observed trend in surface N_2O, and hence the N_2O lifetime is declining. For N_2O, a major greenhouse gas, it means that the climate impact of its anthropogenic emissions will be reduced over this century; and for CFCs where we expect parallel results, it means that these now-banned ozone-depleting gases will be cleaned out of the atmosphere faster. as shown by Butchart and Scaife (2001).

2 Measurements and methods

The Aura MLS observations of N_2O, O_3, and temperature (T) are taken from the Goddard Earth Sciences Data and Information Services Center in the form of Version 5 Level 3 monthly binned profiles from August 2004 through December 2021 (Lambert et al., 2021; Schwartz et al., 2021a, 2021b).   All data are averaged over the 72 longitude bins. There are 43 latitude profiles every 4° (84°S to 84°N). Pressure levels range from 100 to 0.001 hPa with logarithmic spacing, and the resolution depends on the MLS quantity. The very few negative O_3 values (0.04% of data at 0.01 hPa) occur at the minimum in the O_3 profile and

are replaced with the mean value of 0.2 ppm, with negligible impact on photolysis rates. The

negative N_2O values are slightly more frequent (about 0.1% of data at 32 and 22 hPa, but

70   1.6% at 0.5 hPa where the mean value is 2.3 ppb). We do not wish to inflate the N_2O loss by

replace negative values with large positive ones, so we opt for the safest choice and just

replace negative N_2O values with 1 ppb, again, with negligible impact on N_2O loss. The N_2O

vertical grid between 146 and 1 hPa (6 evenly ~~space~~spaced log(pressure) levels per decade) is

coarser than that of O_3 and T (both use ~~the same~~ 12 intervals per decade). The missing N_2O

75   levels in the O_3-T grid are calculated as the square-root of the product of the values on the

adjacent levels. For pressures <0.4 hPa, where MLS V5 N_2O data are ~~lacking~~not reported,

we set the abundance to 0 ppb. ~~Polar areas outside the observations (86° 90°) are included in~~

~~the weighting of the 86° profile. The~~Our consolidated MLS dataset then covers: 43 latitudes

(84°S to 84°N), 37 pressure levels (100 – 0.001 hPa), and 209 months (Aug 2004 to Dec

80   2021).

The observational data consists of 8,987 independent column atmospheres. The top level

(0.001 hPa) is high enough that only a single layer of thickness 0.001 hPa with the same

properties as the top layer is added to complete the atmosphere for the radiative calculation.

85   Below 100 hPa, we add 6 layers with typical tropospheric ~~composition, but~~values (320 ppt),

however, these layers ~~do not much affect the stratospheric~~have negligible impact on N_2O loss

because very little of the critical ~~radiation in these~~ ultraviolet ~~wavelengths~~radiation reaches

below 100 hPa. Each latitude profile is weighted by the area of the ~~troposphere.~~Earth ±2 °

latitude on either side except for latitudes 1 (90 °S-82 °S) and 43 (82 °N-90 °N). For each

90   column we calculate the profile of N_2O loss from photolysis (J-N_2O) and reaction with the

electronically excited atomic oxygen ~~radical~~ $O(^1D)$ from the three reactions:

$$N_2O + h\nu \quad \rightarrow \quad N_2 + O \qquad\qquad (1)$$
$$N_2O + O(^1D) \quad \rightarrow \quad N_2 + O_2 \qquad\qquad (2)$$
95    $$N_2O + O(^1D) \quad \rightarrow \quad NO + NO \qquad\qquad (3)$$
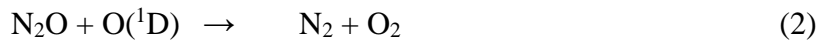
The $O(^1D)$ is calculated from the O_3-T profiles assuming production equals loss

$$O_3 + h\nu \quad \rightarrow \quad O(^1D) + O_2 \qquad\qquad (4)$$
100   $$O(^1D) + N_2 \quad \rightarrow \quad O(^3P) + N_2 \qquad\qquad (5)$$
$$O(^1D) + O_2 \quad \rightarrow \quad O(^3P) + O_2 \qquad\qquad (6)$$
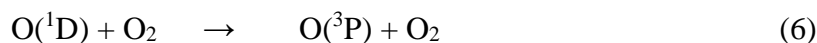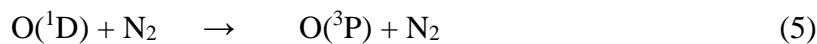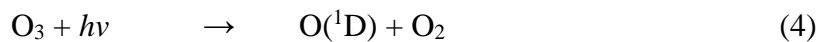
The radiative transfer calculation is the same as in Prather et al. (2015) and includes the solar declination for the middle of each month, the sun-earth distance, but not the solar cycle (a mean solar flux is used). ~~During the MLS Aura record used here, we believe that the solar cycle has had little impact: the~~

~~period 2005-2011 following Cycle 23 showed low activity (smoothed monthly sunspot number < 50); the peak of Cycle 24 (2011-2015) was among the lowest in the last 100 years; and Cycle 25 began in 2020 but activity remained low through 2021. We conclude that the impact of the solar cycle on these observations was much less than the min-to-max decrease in N_2O lifetime of 4-7 % (see P2015) and probably less than 2-3%. Moreover, the symmetry of this low solar activity over 2005-2021 is unlikely to affect trends.~~

Vertically, losses are weighted linearly in pressure (mass); and across latitude, they are weighted by the area of each latitude belt. Annually integrated budgets include the number of days in each month, but leap-years are treated as 365-day years, and thus our annual losses are biased low by 0.07%. Lifetimes are budgetary time scales and calculated as a 12-month burden (TgN) divided by the 12-month loss (TgN/yr). The burden is calculated from monthly-mean, globally-averaged NOAA marine surface measurements (Dlugokencky, 2022) and using the conversion factor of 4.78 TgN/ppb (Prather et al., 2012). Given that the gridding and source files have changed since P2015~~,~~ (which used the 5° latitude GOZCARDS data), we compared the global monthly loss rates for the overlap period with P2015 (Aug 2004 – Dec 2011): the mean difference of 0.2% and rms difference of 0.6% show that both calculations are essentially identical. Uncertainty in the absolute N_2O lifetime is estimated at ±8 % (1-sigma), based primarily on the absolute calibration of MLS N_2O and the chemical kinetics uncertainty, see Section 4 of P2015.

Uncertainties in trends here are calculated from a linear regression of the 12-month running averages of the monthly means as reported or calculated here. We select the 68% (1-sigma) range, because we are looking for 'likely' connections (68% confidence) rather than 'extremely likely' (95%). For example, the linear regression trend in N_2O loss uses the running averages and has 198 monthly points. The uncertainty is scaled up assuming there are only 17 yearly data points. As a check we recalculate the regression fit with the unsmoothed monthly data and get the same uncertainty.

3 Results

The primary calculation here is the annual N$_2$O loss (TgN/yr) shown in Figure 1a. It was
surprising in that such a clear 17-year increase is apparent. Most of the interannual
variability in this 12-month running mean time series is associated with the quasi-biennial
oscillation (see Ruiz et al., 2021). The linear regression gives a trend of +5.0±0.7 %/decade.
This is larger than the +2.9±0.02 %/decade trend in the burden (Figure 1b), and results in an
N$_2$O budgetary lifetime trend of -2.1±0.7 %/decade (Figure 1c). Our best estimate for the
N$_2$O lifetime over the past decade (117 yr) is still close to that in P2015, which included other
model calculations. Most important for the N$_2$O budget is the average loss itself, namely
13.43 TgN/yr with an interannual standard deviation of 3% and min-to-max range of 7%.
The primary source of stratospheric odd-nitrogen species (e.g., NO, NO$_2$, HNO$_3$) is
production of NO in reaction (3), and we calculate the production of NO (Figure 1d), which
(like the N$_2$O loss) also shows a positive trend of +3.9±0.6 %/decade.

The immediate cause of the lifetime trends (i.e., enhanced N$_2$O loss) can be a changean
increase in the photochemical loss frequency, or an increase in the abundance of N$_2$O, or
both. The critical zone for loss in the vertical is 3 to 30 hPa (80% of total loss)), and in
latitude it is 30°S to 30°N (75%), see P2015, and thus. Thus we focus on the tropical middle
stratosphere. Photolysis (reaction 1) dominates loss here (by more than 90%) and the
monthly mean J-N$_2$O at the equator (Figure 1e) shows only a consistent decline across the
critical region from -0.5±0.1 %/decade at the top of the region (3 hPa) to -1.3±0.3 %/decade
at altitudes below 10 hPa. This declinechange by itself would reduce the loss.

The declining J-N$_2$O is clearlyprimarily due to the recovery of overhead ozone during this
period from reduced chlorine-catalyzedcatalysed depletion as the CFCs and other chlorinated
gases have declined following the Montreal Protocol agreement that regulated these source
gases (Bernath et al., 2020; Froidevaux et al., 2022; and references therein). Observations
show continued increases in upper tropical stratospheric ozone for 2000–2020 (Godin-
Beekmann et al., 2022) from a range of satellite measurements, including the MLS O$_3$ used
here that is driving the change of J-N$_2$O. For the upper stratospheric tropics (1-10 hPa), the
generally observed O$_3$ trend of order +1.0 to +1.6 %/decade is consistent with the vertical
pattern and magnitude of the J-N$_2$O trend. ThisAnother source of declining J-N$_2$O is the

170 reduction in photolysis cross sections from lower temperatures. We calculate that the relative change in J in this altitude region is +0.4 %/K, and combining with the observed temperature trend of about -0.5 K/decade (Maycock et al., 2018), we estimate the trend in J from temperature dependent cross sections is -0.2 %/decade and thus a small contribution to the total. The overall trend in J of about -1 %/decade reduces the N_2O loss and makes the

175 disagreement between the burden and loss trends even greater.

Given that N_2O loss is increasing faster than the global burden by +2.1 %/decade, we expect that the N_2O abundances in the critical zone are likewise increasing faster. Because of the reduction in photolysis rates, we expect the abundance to be increasing at about +6 %/decade.

180 Can we see this in the MLS N_2O data? The monthly mean 30°S-30°N N_2O abundances are shown in Figure 1f. The trends are clear but vary over altitude. At the bottom of the critical zone (32 hPa) the trend is negative, -3.4±0.5 %/decade and probably due to a residual negative drift of the V5 MLS data in the lower stratosphere after 2010 as shown in Figure 16 of Livesey et al. (2021). It is unlikely to be real because suppression of vertical transport of

185 N_2O below 30 hPa can hardly lead to increases in N_2O above, and, moreover, the ACE-FTS data show positive trends at these pressures following the analysis of Froidevaux et al. (2022). The trend increases rapidly reaching +5.5±1.2 %/decade in the central zone (10 hPa) and +12.0±2.3 %/decade near the top (4.6 hPa). These increases are used directly in our calculation and average to +6 %/decade needed to explain the trend in total N_2O loss.

190

Are these increases in N_2O real or an artefact of a known calibration drift in the MLS 190 GHz (observations, affecting mainly water vapor and N_2O) observations? The MLS Version 5 dataset benefits from an extensive effort to remove/reduce drifts and verify the MLS H_2O and N_2O against the overlapping ACE-FTS satellite measurements, which are not believed to

195 be drifting (Livesey et al., 2021; Froidevaux et al., 2022). The key comparison is Figure 16 of Livesey et al. (2021). In the tropics (20°S-20°N) there could be a small positive drift in MLS V5 N_2O versus ACE-FTS N_2O for the period 2005-2010 in the range 3-30 hPa, but for the later period 2010-2019, there is no drift, or even a negative drift at 30 hPa and below. This change with altitude may explain the small or negative trend in N_2O below 15 hPa. It is

200 possible that N_2O is increasing throughout the tropical stratosphere if the negative trend at 32 hPa is due to instrumental drift. Parallel analysis of the MLS V4 N_2O (not shown) shows a similar increase in the trend from small negative trends at 32 hPa to large positive ones at 3 hPa (not shown). At the upper end of our range (2.2-6.8 hPa), Froidevaux et al. (2022, their

Figure 12) find similar trends in N_2O to ours (~13 %/decade) from MLS, ACE-FTS, and a model. Their analysis included a much wider latitude range (50°S-50°N), but because N_2O abundances fall off rapidly outside of the tropical ascent region (see Figure 3 of Prather et al., 2015), the tropics should dominate the mean value and its trend. Thus, any calibration drift that impacts the lifetime (i.e., occurring in the critical region 3 to 30 hPa and 30°S to 30°N) is negligible compared to the increasing trend in N_2O loss (+5.0 %/decade). If the drift were slightly negative, correction would further increase this trend.

We believe that the solar cycle has had little impact on N_2O lifetime variability over the MLS Aura record here. The period 2005-2011 following Cycle 23 showed low activity (smoothed monthly sunspot number < 50); the peak of Cycle 24 (2011-2015) was among the lowest in the last 100 years; and Cycle 25 began in 2020 but activity remained low through 2021. We conclude that the impact of the solar cycle on these observations was much less than the min-to-max decrease in N_2O lifetime of 4-7 % (see P2015) and probably less than 2-3%. Moreover, the symmetry of this low solar activity over 2005-2021 is unlikely to affect trends.

4 Implications

The recent WMO Ozone Assessments (Karpechko et al., 2018; Garny et al., 2022) concluded that disagreement remains regarding the direction of the BDC trend between the chemistry-climate model simulations (increasing rates) and the satellite observations of AoA tracers (decreasing or uncertain). We present clear observational evidence supporting the models of what is likely a climate-change driven increase in the net BDC using a major trace gas. N_2O abundances in the tropical upper stratosphere are increasing at rates much faster than tropospheric abundances, but this pattern cannot distinguish between more rapid ascent or reduced mixing with extra-tropical latitudes. The latter would imply a slower growth rate for extra-tropical N_2O, but this is not seen. If we perform a similar trend analysis to that shown in Figure 1f for the extra-tropics (i.e., 30°N-58°N and 30°S-58°S), then we find an almost identical pattern to that in the tropics: increasing at 7-8 %/decade versus 6 at 10 hPa; and at 14-18 %/decade versus 13 at 3.2 hPa, see Supplement Figure S1ab and Table S6. The obvious explanation is an increase in the meridional mean ascent rate in the tropics with little or no change in mixing across the barrier between tropics and extra-tropics. The use of an integrated quantity like the N_2O lifetime provides robust averaging over the large seasonal

and interannual variability of this gas in the middle and upper stratosphere. We expect these results to hold for other gases with mid-stratosphere photolytic sinks, such as CFC-12.

240

Viewing the changing BDC in terms of lifetimes gives a different perspective of the potential consequences of climate change. If this rate of change continues over the 21st century, then the lifetimes of N$_2$O and CFC-12 might drop by 20%. Thus CFCs will be cleared out of the atmosphere earlier than currently projected~~.~~ (e.g., Butchart and Scaife, 2001). The climate

245 impact of N$_2$O emissions will drop because their decay time will fall from 110 yr to 90 yr. Note that the decay time of a pulse based on a lifetime of 117 yr is reduced by a factor of 0.94 due to chemical feedbacks (Prather, 1998; Prather et al., 2015). Overall, we will see an accelerated removal of the long-lived trace gases. ~~The~~Chipperfield et al. (2014) analyzed the change in CFC and N$_2$O atmospheric lifetimes with climate change (year 2100 versus 2000).

250 For the five chemistry-climate models that calculated the N$_2$O lifetime, results were ambiguous: 2 increased, 1 decreased, and 2 were unchanged, all with absolute changes less than 0.5 %/decade. These results are not necessarily inconsistent with the projections here because the modeled scenarios included other chemical changes in the stratosphere and adopted a middling climate scenario (RCP 4.5). Chipperfield et al. also found that AoA

255 metrics were a poor predictor of N$_2$O lifetime (see their Fig. 8-9). Thus, chemistry-climate model intercomparison projects should encourage the calculation of N$_2$O and CFC lifetimes over the 21st century as a ~~straightforward~~major diagnostic of changing BDC~~.~~, although accompanying changes in O$_3$ and T must also be diagnosed to evaluate the photochemically driven changes in lifetime.

260

There is an additional ~~wrinkle~~oddity in this analysis. We find that the production of NO ~~was not~~ (+3.9 %/decade) is increasing faster than the burden (+2.9 %/decade) but not as fast as ~~the~~N$_2$O loss ~~of N$_2$O,~~(+5.0 %/decade), although ~~admittedly~~ the uncertainties overlap. This is expected because NO production peaks lower in the stratosphere and the rapid increase in

265 loss above 10 hPa (~32 km) produces ~~proportional much less NO (see P2015, Figure 1). This~~proportionally much less NO (see P2015, Figure 1). Reduced NO production relative to N$_2$O loss was also a theme in Nevison et al. (1999), who suggested that such changes might occur and be detectable in the observed ratio of NOy (NO and its products) to N$_2$O in the lowermost stratosphere. Our result supports a finding in the analysis of Froidevaux et al.

270 (2022), where the abundance of NO and NO$_2$ in the upper stratosphere is increasing at a rate much less than that of N$_2$O (approximately 2 vs. 12 %/decade~~); however, the~~). The

abundance of NO in the tropical upper stratosphere, however, is a balance between production, vertical transport, and photochemical loss above 40 km, and we cannot ~~be estimated~~estimate it from the production alone. ~~Since this NO production is the cause of O_3 depletion by N_2O in the middle stratosphere, we may find that an enhanced BDC makes N_2O less important as an ozone-depleting gas from both lifetime changes and NO yields.~~

In parallel with our MLS N_2O data analysis, S.E. Strahan led a full chemistry-transport modeling study of the MLS period using the MERRA-2 wind fields and focusing on the chemistry of N_2O, NOy, and O_3. Their results support our analysis and show that more rapid vertical ascent in the tropical upper stratosphere is the cause of enhanced N_2O and N_2O loss. This enhanced transport of NO led to its accumulation in the Arctic upper stratosphere with enhanced O_3 loss there. The modeled changes were shown to be driven by circulation changes, and they were matched by available satellite observations. That paper has now appeared (Strahan et al., 2022).

From the results here and in P2015, we assemble a budget for N_2O from pre-industrial to the last two decades (Table S7). Assuming the pre-industrial loss (11.0 TgN/y) is natural and has remained constant, then the anthropogenic emissions for the 2000s decade is 5.9 TgN/y and that for the 2010s decade is 7.6 TgN/y. This 28 %/decade increase in anthropogenic emissions comes primarily from the increasing N_2O atmospheric burden with only 4 %/decade coming from the decrease in N_2O lifetime derived here. Such growth in emissions shows how hard it will be to control them and identifies N_2O as a looming threat to climate stabilization.

Data Availability. The raw data used here were downloaded from the sites and at the dates specified. The time series calculated here and shown in the figures are included in Tables S1-S5 & S8 in the Supplement.

Supplement. The Supplement related to this article is available online at: https://doi.org/10.5194/acp-22-.....

Author Contributions. MJP designed the research and performed the data analysis. LF and NJL analysed the accuracy of the datasets. MJP wrote the paper. LF and NJL reviewed and edited the paper.

Competing interests. The contact author has declared that neither they nor their co-authors have any competing interests

310 *Acknowledgments*. We thank J.L. Neu for helpful framing discussions and other MLS team members (Alyn Lambert, William Read, and Ryan Fuller) who contributed to the MLS v4 and v5 data sets used here (O_3, T, and especially N_2O). We also thank the two anonymous ACP reviewers whose constructive reviews have improved the manuscript.

315 *Financial support*. Research at the University of California Irvine was supported by grants from the National Aeronautics and Space Administration's Atmospheric Chemistry Modeling and Analysis Program (ACMAP; grant no. 80NSSC21K1454) and the National Science Foundation's Atmospheric Chemistry Program (grant no. AGS-2135749). Work at the Jet Propulsion Laboratory was performed under contract with NASA (80NM0018D0004).

320

References

Abalos, M., Calvo, N., Benito-Barca, S., Garny, H., Hardiman, S. C., Lin, P., Andrews, M. B., Butchart, N., Garcia, R., Orbe, C., Saint-Martin, D., Watanabe, S., and Yoshida, K.: The Brewer–Dobson circulation in CMIP6, Atmos. Chem. Phys., 21, 13571–13591,
325   https://doi.org/10.5194/acp-21-13571-2021, 2021.
Bernath P. F., Steffen J., Crouse J., and Boone C. D.: Sixteen-year trends in atmospheric trace gases from orbit, J. Quant. Spectrosc. Ra. 253, 107178, https://doi.org/10.1016/j.jqsrt.2020.107178, 2020.
Butchart, N. (2014), The Brewer-Dobson circulation, Rev. Geophys.,52, 157–184,
330   doi:10.1002/2013RG000448.
Butchart, N., Scaife, A.: Removal of chlorofluorocarbons by increased mass exchange between the stratosphere and troposphere in a changing climate. Nature 410, 799–802, https://doi.org/10.1038/35071047, 2001.
Chipperfield, M.P., Q. Liang, S.E. Strahan, O. Morgenstern, S.S. Dhomse, N.L. Abraham,
335   A.T. Archibald, S. Bekki, P. Braesicke, G. Di Genova, E.L. Fleming, S.C. Hardiman, D. Iachetti, C.H. Jackman, D.E. Kinnison, M. Marchand, G. Pitari, J.A. Pyle, E. Rozanov, A. Stenke and F. Tummon, Multi-model estimates of atmospheric lifetimes of long-lived Ozone-Depleting Substances: Present and future, J. Geophys. Res., 119, 2555-2573, doi:10.1002/2013JD021097, 2014.
340 Dlugokencky, E. (2022) Data from the NOAA web site, www.esrl.noaa.gov/gmd/ccgg/trends_n2o/ n2o_mm_gl.txt [pulled 2022-07-26], ed.dlugokencky@noaa.gov
Fritsch, F., Garny, H., Engel, A., Bönisch, H., and Eichinger, R.: Sensitivity of age of air trends to the derivation method for non-linear increasing inert SF6, Atmos. Chem. Phys.,
345   20, 8709–8725, https://doi.org/10.5194/acp-20-8709-2020, 2020.
Froidevaux, L., Kinnison, D. E., Wang, R., Anderson, J., and Fuller, R. A.: Evaluation of CESM1 (WACCM) free-running and specified dynamics atmospheric composition

simulations using global multispecies satellite data records, Atmos. Chem. Phys., 19, 4783–4821, https://doi.org/10.5194/acp-19-4783-2019, 2019.

350 Froidevaux, L., Kinnison, D. E., Santee, M. L., Millán, L. F., Livesey, N. J., Read, W. G., Bardeen, C. G., Orlando, J. J., and Fuller, R. A.: Upper stratospheric ClO and HOCl trends (2005–2020): Aura Microwave Limb Sounder and model results, Atmos. Chem. Phys., 22, 4779–4799, https://doi.org/10.5194/acp-22-4779-2022, 2022.

Garny, H., H. Hendon (Lead Authors), M. Abalos, G. Chiodo, A. Purich, W. Randel K. Smith
355 and D. Thompson, Scientific Assessment of Ozone Depletion: 2022, World Meteorological Organisation Global Ozone Research and Monitoring Project-Report No. XX, WMO/UNEP Scientific Assessment of Ozone Depletion: 2022. Chapter 5: Stratospheric Ozone Changes and Climate, World Meteorological Organization, Geneva, Switzerland, 2022.

360 Godin-Beekmann, S., Azouz, N., Sofieva, V., Hubert, D., Petropavlovskikh, I., Effertz, P., Ancellet, G., Degenstein, D., Zawada, D., Froidevaux, L., Frith, S., Wild, J., Davis, S., Steinbrecht, W., Leblanc, T., Querel, R., Tourpali, K., Damadeo, R., Maillard-Barras, E., Stübi, R., Vigouroux, C., Arosio, C., Nedoluha, G., Boyd, I., and van Malderen, R.: Updated trends of the stratospheric ozone vertical distribution in the 60° S–60° N
365 latitude range based on the LOTUS regression model, Atmos. Chem. Phys. Discuss. [preprint], https://doi.org/10.5194/acp-2022-137, accepted, 2022.

Karpechko, A., A. Maycock (Lead Authors), M. Abalos, J. Arblaster, H. Akiyoshi, C. Garfinkel, K. Rosenlof and M. Sigmond, Scientific Assessment of Ozone Depletion: 2018, World Meteorological Organisation Global Ozone Research and Monitoring
370 Project-Report No. 58, WMO/UNEP Scientific Assessment of Ozone Depletion: 2018. Chapter 5: Stratospheric Ozone Changes and Climate, World Meteorological Organization, Geneva, Switzerland, 2018.

Lambert, A., Livesey, N., Read, W., and Fuller, R., MLS/Aura Level 3 Monthly Binned Nitrous Oxide (N2O) Mixing Ratio on Assorted Grids V005, Greenbelt, MD, USA,
375 Goddard Earth Sciences Data and Information Services Center (GES DISC), Accessed: [2022-05-06], 10.5067/Aura/MLS/DATA/3545, 2021.

Livesey, N. J., Read, W. G., Froidevaux, L., Lambert, A., Santee, M. L., Schwartz, M. J., Millán, L. F., Jarnot, R. F., Wagner, P. A., Hurst, D. F., Walker, K. A., Sheese, P. E., and Nedoluha, G. E.: Investigation and amelioration of long-term instrumental drifts in water
380 vapor and nitrous oxide measurements from the Aura Microwave Limb Sounder (MLS) and their implications for studies of variability and trends, Atmos. Chem. Phys., 21, 15409–15430, https://doi.org/10.5194/acp-21-15409-2021, 2021.

Maycock, A. C., Randel, W. J., Steiner, A. K., Karpechko, A. Y., Christy, J., Saunders, R., et al.: Revisiting the mystery of recent stratospheric temperature trends. Geophysical
385 Research Letters, 45, 9919–9933. https://doi.org/10.1029/2018GL078035, 2018.

Neu, J. L., and Plumb, R. A., Age of air in a "leaky pipe" model of stratospheric transport, J. Geophys. Res., 104(D16), 19243– 19255, doi:10.1029/1999JD900251, 1999.

Nevison, C.D., Keim, E.R., Solomon, S., Fahey, D.W., Elkins, J.W., Lowenstein, M., Podolske, J.R.: Constraints on N_2O sinks inferred from observed tracer correlations in
390 the lower stratosphere, Global Biogeochemical Cycles, 13(3) 737-742, 1999.

Plumb, R. A., and J. D. Mahlman, The zonally-averaged transport characteristics of the GFDL general circulation/tracer model, J. Atmos. Sci.,44, 298–327, doi: 10.1175/1520-0469(1987)044%3C0298:TZATCO%3E2.0.CO;2, 1987.

Prather, M.J., Time scales in atmospheric chemistry: coupled perturbations to N2O, NOy,
395 and O3, Science, 279, 1339-1341, 1998.

Prather, M.J., C.D. Holmes, and J. Hsu, Reactive greenhouse gas scenarios: Systematic exploration of uncertainties and the role of atmospheric chemistry, Geophys. Res. Lett., 39, L09803, 5 pp., doi:10.1029/2012GL051440, 2012.

Prather, M.J., J. Hsu, N.M. DeLuca, C.H. Jackman, L.D. Oman, A.R. Douglass, E.L. Fleming, S.E. Strahan, and S.D. Steenrod, O.A. Søvde, I.S.A. Isaksen, L. Froidevaux, and B. Funke Measuring and modeling the lifetime of nitrous oxide including its variability, J. Geophys. Res. Atmos., 120, 5693–5705. doi: 10.1002/2015JD023267, 2015.

Ruiz, Daniel J., Michael J. Prather, Susan E. Strahan, Rona L. Thompson, Lucien Froidevaux, Stephen D. Steenrod, How atmospheric chemistry and transport drive surface variability of N2O and CFC-11. J. Geophys. Res.: Atmospheres, 126, e2020JD033979. https://doi.org/10.1029/2020JD033979, 2021.

Schwartz, M., Livesey, N., Read, W., and Fuller, R., MLS/Aura Level 3 Monthly Binned Temperature on Assorted Grids V005, Greenbelt, MD, USA, Goddard Earth Sciences Data and Information Services Center (GES DISC), Accessed: [2022-07-26] [Data Access Date], 10.5067/Aura/MLS/DATA/3550, 2021a.

Schwartz, M., Froidevaux, L., Livesey, N., Read, W., and Fuller, R., MLS/Aura Level 3 Monthly Binned Ozone (O3) Mixing Ratio on Assorted Grids V005, Greenbelt, MD, USA, Goddard Earth Sciences Data and Information Services Center (GES DISC), Accessed: [2022-05-06, yrs 2004 & 2021 re-pulled on 2022-07-06], 10.5067/Aura/MLS/DATA/3546, 2021b.

Strahan, S. E., Coy, L., Douglass, A. R., & Damon, M. R.: Faster tropical upper stratospheric upwelling drives changes in ozone chemistry. Geophys. Res, Letts., 49, e2022GL101075, https://doi.org/10.1029/2022GL101075, 2022
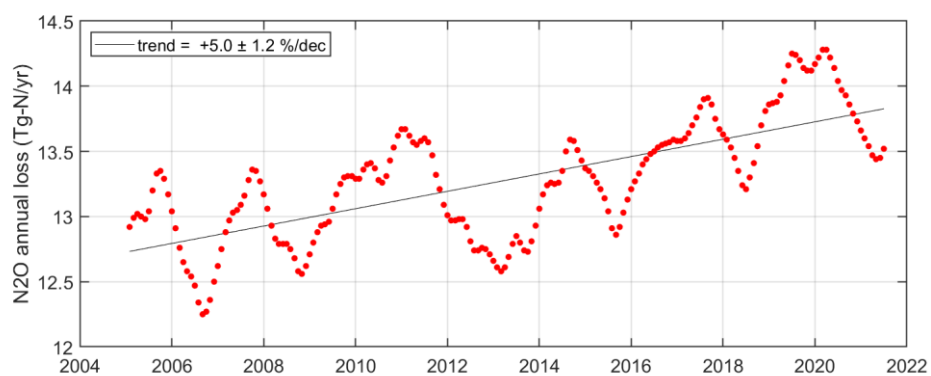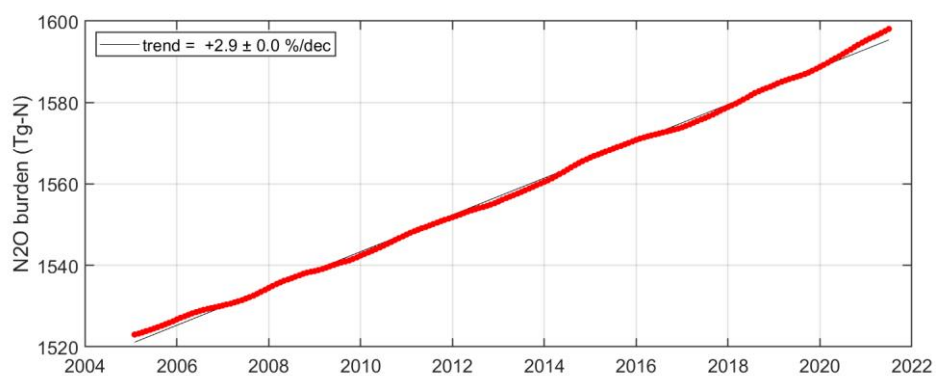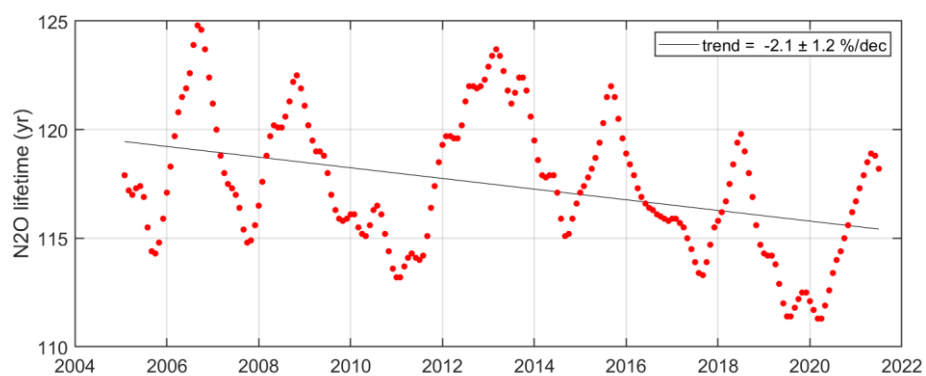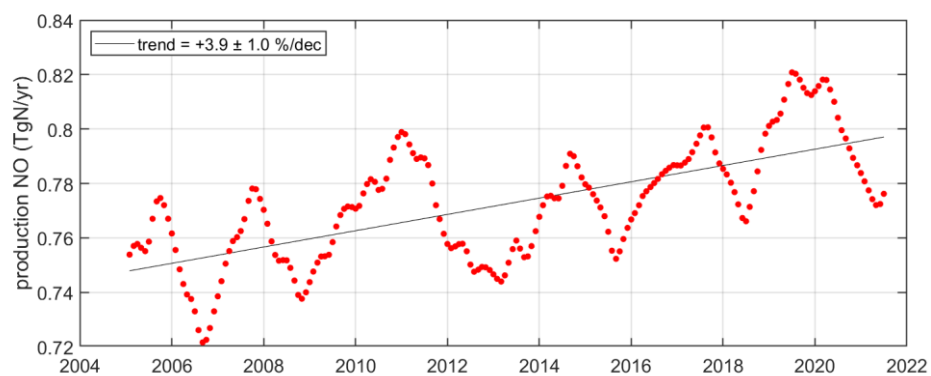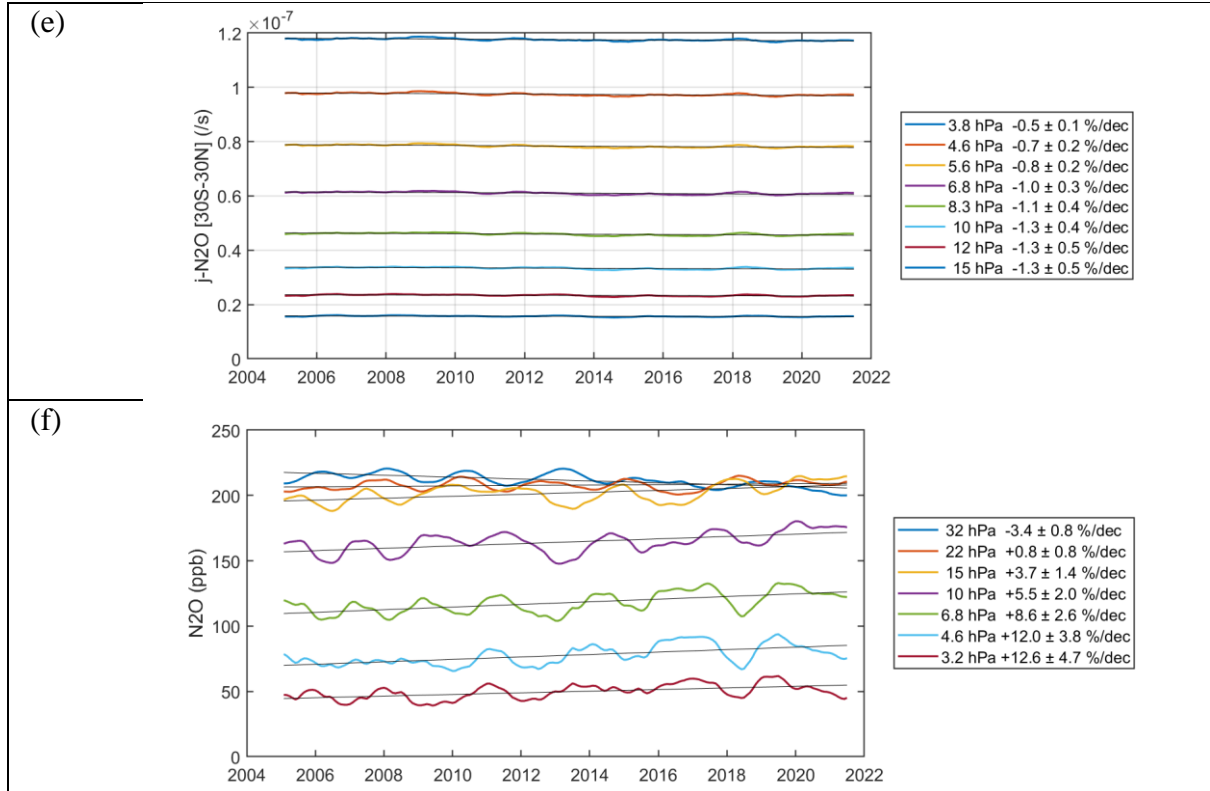
Figure 1. (a) N_2O loss rate (TgN/yr) as monthly values of a 12-month running mean. The 198 red points begin with the 12-month average of August 2004 through July 2005 plotted as February 1, 2005 with the final point being July 1, 2021 (all of 2021). The thin black trend line show the slope and uncertainty in the legend, see text. (b) N_2O global burden (TgN) based on marine surface observations. (c) N_2O lifetime derived from the burden divided by loss rate. (d) Production of NO (TgN/yr) from N_2O loss. (e) Stratospheric photolysis rates, j-N_2O (/s), at the standard MLS V5 T pressure levels (see legend) and averaged over 30°S-30°N. (f) N_2O abundance (ppb) at the standard V5 N_2O pressure levels (see legend) and averaged over 30°S-30°N.